EPR and DFT Study on the Stabilization of Radiation-Generated Methyl Radicals in Dehydrated Na-A Zeolite

Marek Danilczuk,*,†,‡ Dariusz Pogocki,†,§ Anders Lund,‡ and Jacek Michalik†

Institute of Nuclear Chemistry and Technology, Dorodna 16, 03-195 Warsaw, Poland, Department of Physics, Chemistry and Biology, IFM, Linköping University, S-581 83 Linköping, Sweden, and Faculty of Chemistry, Department of Biochemistry and Biotechnology, Rzeszów University of Technology, 6 Powstańców Warszawy Ave. 35-959, Rzeszów, Poland

Received: June 6, 2006; In Final Form: August 17, 2006

Electron paramagnetic resonance (EPR) spectroscopy was applied to study paramagnetic species stabilized in Na-A zeolite exposed to gaseous methane and γ-irradiated at 77 K. Two types of EPR spectra were recorded during thermal annealing of zeolite up to room temperature. Owing to the results for the zeolite exposed to $^{13}CH_4$ the multiplet observed at 110 K was assigned to a $^{\bullet}CH_3\cdots Na^+$ complex. After decay of the multiplet, the isotropic quartet of methyl radical was recorded in the temperature range of 170−280 K. On the basis of the EPR parameters it is postulated that $^{\bullet}CH_3$ radicals in this temperature region are able to freely rotate inside the zeolite cage. The structures of the $^{\bullet}CH_3\cdots Na^+$ adsorption complex and respective hyperfine coupling constants were calculated by applying DFT quantum chemical methods. Two different models were applied to represent the zeolite framework: the 6T structure of one six-membered ring and the 3T cluster. The hyperfine coupling constants calculated for the $^{\bullet}CH_3\cdots Na^+$ adsorption complex for both applied models show very good agreement with those obtained experimentally.

Introduction

Recent research has shown that the porous nature of zeolite plays a significant role in the separation and stabilization of various reactive intermediates as atoms, radicals, radical ions, and clusters.[1−4] The studies of such intermediates are very important for better understanding of the mechanisms of chemical reactions in heterogeneous catalysis, photochemistry, and radiation chemistry and biology.[5−8] Recently, metal loaded zeolites were found to be promising catalysts in the decomposition of automotive exhaust emission.[9] Synthetic zeolites play important roles in petrochemistry enabling catalytic conversion of hydrocarbons to the liquid fuels.[10]

The nature of the reactive paramagnetic intermediates in irradiated hydrocarbons in frozen solutions as well as in liquid phase and inert gas matrices has been studied by the EPR technique for some 40 years.[11−13] By applying EPR spectroscopy for in situ irradiated hydrocarbons the radiation-induced methyl radicals can be studied also in the liquid phase, however, only over a quite narrow temperature range, i.e., 90−120 K.[18] At higher temperatures methyl radicals can be observed when adsorbed on solid surfaces such as porous Vycor glass.[14,15] The EPR signal of $^{\bullet}CH_3$ adsorbed on a solid surface usually shows an asymmetric line profile.[16,17]

Methyl radicals observed spectroscopically in solution and in inert gas matrices at low temperature seem to have quite high leeway of tumbling.[18] The EPR shows for them an isotropic quartet with 1:3:3:1 intensity ratio and hyperfine splitting of 2.3023 mT. For ^{13}C enriched compounds the hyperfine splitting of ^{13}C is equal to 3.834 mT. On the contrary, methyl radicals adsorbed on the surface of silica have a proton hyperfine splitting of about 2 mT, significantly smaller than that of freely tumbling methyl radicals. This decrease has been associated with changes of their electronic structure, which depends on the nature of the adsorption sites.[19−21]

In contrast to methyl radicals adsorbed on solid surfaces, the EPR spectra of $^{\bullet}CH_3$ radicals stabilized in zeolite cages and channels usually have an isotropic character and a line intensity ratio 1:3:3:1 similar to spectra observed in liquid methane.[18]

The methyl radicals trapped in zeolite frameworks can be stabilized for longer periods than on solid surfaces at low temperature. Noble et al. investigated methyl radicals stabilized in γ-irradiated A zeolite. Below 90 K several types of radicals were detected but the methyl radical was the most stable. An interesting feature of the methyl radicals stabilized in zeolite A was the apparent doublet nature of the low and high field transition ($m = \pm^3/_2$). A possible explanation is that two radicals with the same coupling constants are characterized by different *g* factors but in this case all lines not only the outermost should be shifted equally. The asymmetric profile of the outer lines in the spectrum of the methyl radical can better be explained as a result of slight anisotropy of hyperfine interaction.[22]

A similar system has been investigated by Shiotani et al. They detected three types of methyl radicals depending on activation temperature. The first "normal" one was characterized by isotropic EPR parameters, the second one had a splitting with an additional proton, and the third one exhibited a large splitting due to one of the three protons.[23]

The effects of stabilization of methyl radicals in the zeolite frameworks are substantial; their lifetime in zeolites at room temperature could be extended even up to hours whereas in liquid hydrocarbons alkyl radicals can live only for several microseconds.[24]

* Address correspondence to this author at the Institute of Nuclear Chemistry and Technology. Fax: +48-22-8111532. Phone: +48-22-8112347. E-mail: mdan@ichtj.waw.pl.

† Institute of Nuclear Chemistry and Technology.

‡ Linköping University.

§ Rzeszów University of Technology.

10.1021/jp063506y CCC: $33.50
Published on Web 11/11/2006

The manner of stabilization of the precursors of radiation-generated alkyl radicals, i.e., of the adsorbed hydrocarbons, has also aroused research interest. Literature data clearly show that in zeolites hydrocarbon molecules are adsorbed in the vicinity of Brönsted acid sites and/or exchangeable cations.[25,26] The adsorbate transition complex of methane molecules with a model cluster of bridging OH groups has been investigated both theoretically and experimentally.[27,28] The results collected so far suggest that the most stable binding geometry of the methane−zeolite complex is achieved through physisorption of methane in the bridging hydroxyl group via two hydrogen bonds.

The application of quantum chemistry methods can here provide important information on the nature of the adsorbate−zeolite interaction. Particularly the electronic and magnetic properties of the intermolecular adsorption complex can be predicted with a satisfactory accuracy. For example, the interpretation of hyperfine coupling constants by theoretical calculations can often help to rationalize the experimental results.

However, due to the complexity of adsorbate−zeolite systems, the application of very sophisticated ab initio or density functional theory (DFT) methods for the calculations of hyperfine coupling constants has until recently been limited to rather simple systems[29] as these methods require quite substantial computational effort. Semiempirical methods were therefore extensively and often successfully employed to model such systems in the past.[30,31] Just recently, with the advent of new-generation computers, more accurate quantum chemical studies on those systems have started to appear in the literature.[32,33] To limit the computational demand calculations are still performed for rather small fragments of zeolite cages or channels.

The literature data univocally suggest that combination of hybrid functional DFT methods with Pople-type Gaussian basis sets gives appropriate information on the structure of examined molecules. Especially, the B3LYP/6-31G(d) level of calculations gives geometries with sufficient quality for a broad range of chemical applications. Most importantly, application of DFT methods for computing magnetic parameters of different types of organic radicals was been shown to give hyperfine couplings close to experimental data.[34−39] In particular, the basis sets EPR-II and EPR-III designed by Barone[40] for the calculation of magnetic properties of radicals in conjunction with the application of the B3LYP[41] functional reproduce experimental hyperfine coupling constants for H, C, and N in a number of radicals with an error usually smaller than 10%. The error here is comparable with that, which in the interpretation of experimental data usually corresponds to uncertainty related to an arbitrary choice of the line shape (Gaussian or Lorentzian) during the nonlinear fitting.

Experimental Section

Linde 4A zeolite was supplied by Linde Air Products Company. The normal methane CH_4 of 99.0% purity and the 99.0% ^{13}C enriched methane, $^{13}CH_4$, were purchased from Aldrich Chemical Co. and were used without further purification.

The Na-A zeolite samples were placed into Suprasil EPR tubes equipped with stopcocks and dehydrated in vacuo gradually raising the temperature up to 473 K for 4 h. Next the samples were oxidized at 573 K for 3 h with O_2 under the static pressure of 80 kPa. Thereafter oxygen was pumped off at the same temperature for 1 h.

The adsorption of methane was carried out at room temperature under pressures of 0.4, 3, 13, and 25 kPa for 24 h. To check the effect of adsorption temperature on the stabilization of methyl radicals, samples already exposed to CH_4 were heated at 353, 413, and 473 K for 1 h. Then the excess of methane was shortly pumped off and the zeolite samples were irradiated in a ^{60}Co-source at liquid nitrogen temperature (77 K) with a dose of 5 kGy.

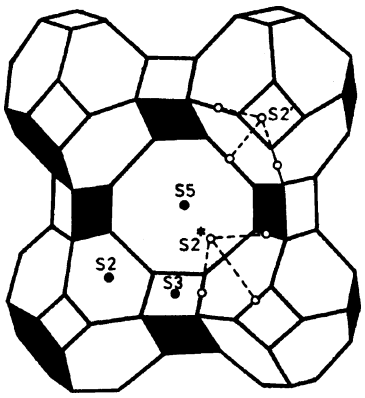

Figure 1. Schematic diagram of the zeolite A structure. Each vertex represents an Al or Si atom and the lines represent O bridges.

The EPR spectra were recorded with an X-band Bruker ESP 300E spectrometer equipped with a liquid nitrogen cryostat. The temperature of the sample during EPR measurements was controlled by a Bruker variable temperature unit in the temperature range 110−310 K. *g*-Values were determined by using a DPPH specimen for field calibration.

Methods of Computation. Two different models have been applied to represent the zeolite framework: the 6T structure of one six-membered ring and the 3T cluster ($H_3SiOAl(OH)_2OSiH_3$) retaining a fragment of an octagonal window terminated with hydrogen atoms and with an embedded sodium cation. Geometries of the two model complexes have been fully optimized at the B3LYP level with the LANL2DZ[42−44] basis set. Calculations of hyperfine coupling constants have been carried out in single-point runs with the DGDZVP and DGauss A1 Coulomb Fitting basis sets for the sodium atom and with EPR-III for hydrogen and carbon atoms of the methyl radical. This approach has been proven to give reliable results for the silver−diethylene complex stabilized in SAPO-11 molecular sieve.[29] All calculations have been performed with the Gaussian′03 suite of programs.[45]

Structure of Zeolite A.[46] In zeolite A alumina and silica tetrahedra are bonded together to form truncated octahedra called β-cages or sodalite units with a diameter of 1.14 nm, which constitutes the channel structure of zeolite A (Figure 1). The entrance of organic adsorbates to a sodalite unit from an α-cage is only possible through a six-membered ring, called a hexagonal window. Its diameter of 0.22 nm is too small to let organic adsorbate get into sodalite. Whereas Na^+ cations in A zeolite occupy preferentially S2′ sites inside β-cages they may also be located at S2 and S* sites in α-cages (see Figure 1). The framework of zeolite A consists of one α and eight β cages per unit cell. The cation capacity of zeolite A is 12 cations per unit cell.

Results and Discussion

The EPR spectra of γ-irradiated Na-A zeolite are shown in Figure 2. Asymmetric singlet **a** is attributed to radiation induced damages in the zeolite framework—a hole located between oxygen and silicon atoms (Figure 2a). A similar signal was detected in Na-Y zeolite.[22,47] The experimental and simulated EPR spectra of γ-irradiated Na-A zeolite containing methane adsorbed at a pressure of 0.4 kPa at room temperature are shown

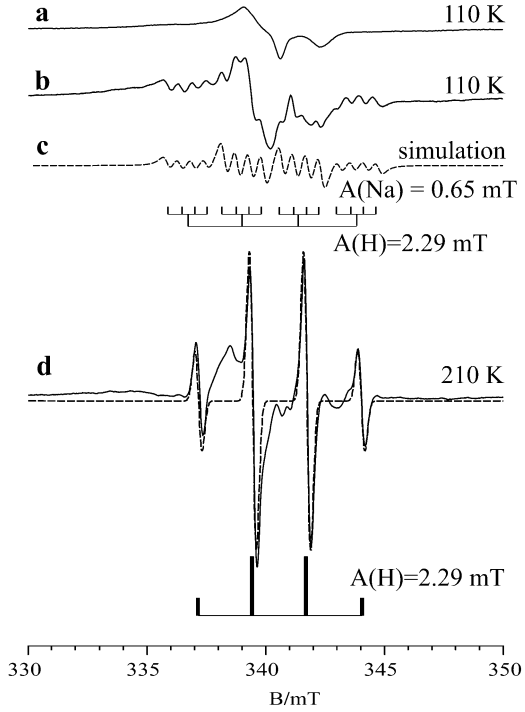

Figure 2. EPR spectra of (a) dehydrated Na-A zeolite recorded at 110 K, (b) dehydrated Na-A/CH_4 zeolite recorded at 110 K, (c) a simulated spectrum of the $^{\bullet}CH_3\cdots Na^+$ complex, and (d) $^{\bullet}CH_3$ methyl radical observed in dehydrated Na-A/CH_4 zeolite at 210 K (the dashed line represents the simulated spectrum).

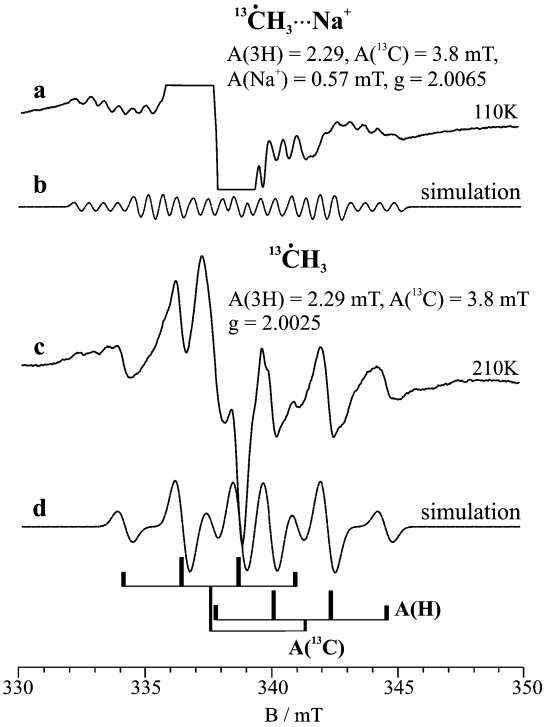

Figure 3. EPR spectra of (a) dehydrated Na-A/$^{13}CH_4$ zeolite recorded at 110 K, (b) a simulated spectrum of the $^{\bullet 13}CH_3\cdots Na^+$ complex, (c) the $^{\bullet 13}CH_3$ methyl radical observed in dehydrated zeolite Na-A/$^{13}CH_4$ at 210 K, and (d) a simulated spectrum of the $^{\bullet 13}CH_3$ methyl radical.

in Figure 2b−d. At 110 K the EPR signal is composed of two sets of lines: an anisotropic singlet **a** analogical with those detected in zeolite without adsorbates derived from radiation induced damage in the Na-A zeolite framework and a lower intensity multiplet **b**. After computer analysis of this spectrum we concluded that signal **b** consists of four groups of lines separated by 2.29 mT and centered at $g = 2.0056$. Each group is composed of four isotropic lines split by 0.65 mT (Figure 2c). The assignment of this signal is discussed below.

During thermal annealing above 170 K a new EPR signal appears: an isotropic quartet **d** with intensity rations 1:3:3:1, $A = 2.29$ mT, and $g = 2.0023$. The signal reaches the highest intensity at 210 K and remains stable until 280 K (Figure 2d). The dashed line profile in Figure 2d shows a $^{\bullet}CH_3$ spectrum simulated with the following Hamiltonian parameters: $A = 2.29$ mT, $g = 2.0023$, $\Delta H_{pp} = 0.3$ mT, and Gaussian line shape. The simulation parameters are in good agreement with the EPR parameters of methyl radicals observed in liquid methane at 196 K.[12] This prompts us to conclude that the quartet **d** represents $^{\bullet}CH_3$ radicals which are not adsorbed on the surface of the zeolite framework but rather freely rotate in the void of zeolite cages.

The CH_4 molecules are too big to migrate into the β-cages through hexagonal windows of diameter ca. 0.22 nm. Therefore, it seems reasonable to assume that after adsorption at room temperature CH_4 molecules are present only in α-cages and methyl radicals generated radiolytically at 77 K are also trapped there. At lower temperature methane is adsorbed and located close to the exchangeable cations. At higher temperature the mobility of methane and methyl radical increases and molecules migrate to the cage center. Diffusion of radicals between the cages takes place above 280 K. As a result $^{\bullet}CH_3$ radicals decay in radical−radical reactions.

The experimental and simulated spectra of γ-irradiated Na-A zeolite containing $^{13}CH_4$ methane adsorbed at a pressure of 0.4 kPa recorded at 110 and 210 K are shown in Figure 3. The spectrum at 110 K consists of the dominating signal from radiation-induced damage in the Na-A zeolite framework overlapped with a low-intensity multiplet **a** (Figure 3a). The multiplet was successfully simulated with the following Hamiltonian parameters $A(^{13}C) = 3.85$ mT, $A(3H) = 2.3$ mT, $A(Na^+) = 0.65$ mT, $g = 2.0065$, and $\Delta H_{pp} = 0.33$ mT (Figure 3b). The simulation clearly indicates that the additional structure of the $^{\bullet 13}CH_3$ radical is due to the interaction with Na^+ ($I = 3/2$) cation and not with the methane molecules or methane derived species, for example, methyl radical cations. Because the accessible cation sites are mostly located in the vicinity of hexagonal windows connecting α- and β-cages we hypothesize (see below) that at low temperature the $^{\bullet}CH_3$ radical in an α-cage interacts with a Na^+ cation at S2 sites in the vicinity of the hexagonal window (Figure 1). The $^{\bullet}CH_3\cdots Na^+$ signal is only recorded in the temperature range 77−110 K when mobility of radicals is very low. This strongly suggests that after adsorption CH_4 molecules form a diamagnetic complex. During radiolysis the $CH_4\cdots Na^+$ complex is transformed to a paramagnetic one by hydrogen abstraction from the methane molecule.

During thermal annealing the spectral changes for the Na-A/$^{13}CH_4$ zeolite follow the transformations observed earlier in the Na-A/$^{12}CH_4$ sample. Above 170 K the multiline spectrum **a** decays and a doublet of quartets **c** starts appearing. It is observable in the same temperature range as the $^{\bullet}CH_3$ quartet in Na-A/$^{12}CH_4$ zeolite. The spectrum **c** was successfully simulated with the following Hamiltonian parameters and is shown in Figure 3d: $A(^{13}C) = 3.85$ mT, $A(3H) = 2.29$ mT, $g = 2.0025$, and $\Delta H_{pp} = 0.46$ mT, assuming Gaussian line shape.

A similar experiment was performed with methane adsorbed on a zeolite sample fully exchanged with Li^+ cation. The spectra of γ-irradiated Li-A zeolite containing CH_4 adsorbed at a pressure of 0.4 kPa and recorded at 110 and 210 K are shown in Figure 4. At 110 K only the signal derived from radiation-

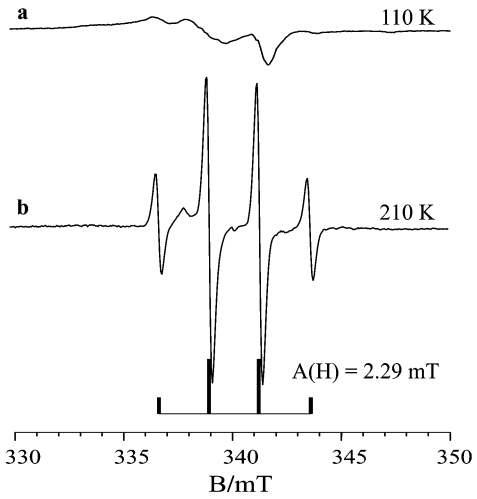

Figure 4. EPR spectra of (a) dehydrated Li-A zeolite recorded at 110 K and (b) dehydrated zeolite Li-A/CH_4 recorded at 210 K.

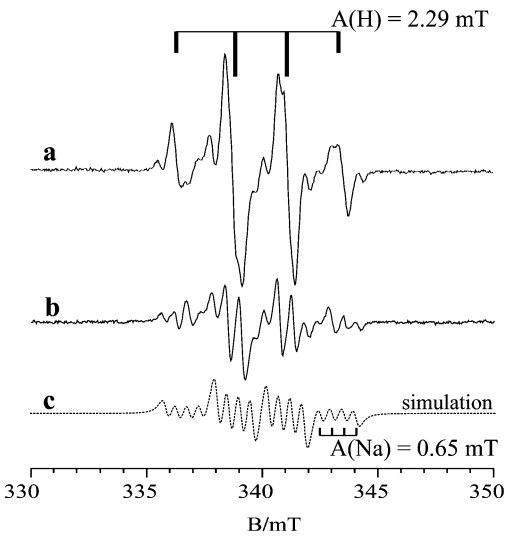

Figure 5. Result of deconvolution of the EPR spectrum of Na-A/CH_4 zeolite. Methane was adsorbed at 413 K, γ-irradiation was performed at 77 K. (a) Result of subtraction of the EPR signal of radiation-induced centers in dehydrated zeolite from the experimental spectrum of zeolite exposed to methane at 413 K. (b) Spectrum obtained by subtraction of the quartet of the freely rotating $^{\bullet}CH_3$ radical from spectrum a. (c) Simulated spectrum of the $^{\bullet}CH_3\cdots Na^+$ complex (A(3H) = 2.29 mT, A(Na) = 0.65 mT).

induced damage in the zeolite framework is detected. After thermal annealing above 170 K an isotropic quartet identical with that detected in Na-A/CH_4 with intensity ratio 1:3:3:1, A = 2.29 mT, and g = 2.0023 appeared. The signal reaches the highest intensity at 210 K and is still observed at 280 K. These results strongly suggest that low intense multiplets observed in Na-A/CH_4 and Na-A/$^{13}CH_4$ samples represent the $^{\bullet}CH_3\cdots Na^+$ complex and are not observed when the Na^+ cation is replaced with Li^+.

When zeolite samples with adsorbed methane are heated before irradiation the EPR signal due to sodium−methyl complex shows bigger intensity and stability. Then the signal of the complex is clearly seen above 200 K overlapping with the quartet of the freely rotating $^{\bullet}CH_3$ radical. The stability of the $^{\bullet}CH_3\cdots Na^+$ complex increases with the temperature of zeolite heating and reaches a maximum for samples preheated at 413 K. The EPR spectrum of such sample recorded after irradiation at 210 K was deconvoluted and the results of that procedure are presented in Figure 5. The spectrum **a** is the result of subtraction of the EPR signal of radiation-induced centers in dehydrated zeolite from the experimental spectrum of zeolite exposed to methane at 413 K. The spectrum **b** was obtained by subtraction of the quartet of the freely rotating $^{\bullet}CH_3$ radical from spectrum **a**. The multiplet **b**, a quartet of quartets (Figure 5b), has been simulated as **c** with spin Hamiltonian parameters (A(3H) = 2.29 mT, A(Na^+) = 0.65 mT) identical with the parameters of spectrum **c** in Figure 2, previously assigned to the $^{\bullet}CH_3$ radical interacting with the Na^+ cation. In the sample heated at 413 K the $^{\bullet}CH_3\cdots Na^+$ complex is more stable and its EPR spectrum was observed even at room temperature. This strongly suggests that in zeolite preheated with adsorbed CH_4 molecules the diamagnetic precursor of the paramagnetic complex occupies a different site than in zeolites exposed to methane at room temperature. We postulate that at elevated temperatures some CH_4 molecules are able to penetrate hexagonal windows and get into β-cages where they form a complex with the inner Na^+ cations at S2′ sites. The β-cage $^{\bullet}CH_3\cdots Na^+$ complex should be more stable than the α-cage complex because below room temperature $^{\bullet}CH_3$ radicals are unable to migrate through the hexagonal window to the wide channels connecting the α-cages.

There is no direct evidence that methane molecules could gain access to the β cavities. However, in a crystallographic study of zeolite A containing Xe, which is about the same size as methane molecules, a Xe molecule was always found in the center of sodalite β, indicating that passage of Xe atoms through the hexagonal window is due to dynamic processes at higher temperature.[48,49]

The EPR spectra of γ-irradiated Na-A/CH_4 zeolite do not depend much on the pressure of adsorbed methane. The EPR parameters and temperature transformation of EPR signals are almost identical for methane pressures in the range 0.4−13 kPa except for the line width, which increases from 0.3 mT for 0.4 kPa of CH_4 to 0.58 mT for 13 kPa. The observed effect might be due to the dipolar interaction of the unpaired electron with protons of CH_4 molecules located closer to $^{\bullet}CH_3$ radicals in the samples exposed to higher CH_4 pressure. The lower stability of $^{\bullet}CH_3$ radicals in zeolite exposed to higher CH_4 pressure supports this hypothesis. In the samples with 0.4 kPa of CH_4 methyl radicals are still observed at room temperature whereas for 2.6 kPa and higher pressure they decay below 230 K presumably by the reactions with CH_4 molecules situated in the same zeolite cage.

No other paramagnetic products were detected in any of the samples when the signal of $^{\bullet}CH_3$ disappeared. In contrast to our results Noble et al. reported formation of several other types of radicals in addition to the methyl radical, with hyperfine splitting constants of 2.19 mT on the surface of zeolite Na-A below 90 K.[22] In our study the EPR spectrum of methyl radicals is still observed even at 280 K and has a completely isotropic line profile. The EPR parameters are similar to parameters of $^{\bullet}CH_3$ radicals observed in the liquid hydrocarbons. This suggests that $^{\bullet}CH_3$ is stabilized in the void of an α-cage and is not interacting with the surface of the zeolite.

Shiotani et al. have shown that depending on the activation temperature different types of methyl radicals are stabilized in zeolite Na-A. Besides the normal methyl radical, formation of two additional $^{\bullet}CH_3$ radicals has been reported: one with a splitting from an additional proton, and a second with an extremely large splitting from one of the three protons. Even in the samples activated at high temperature (250 °C) no signals showing interaction of the paramagnetic products of methane radiolysis with Na^+ cation were detected.[23]

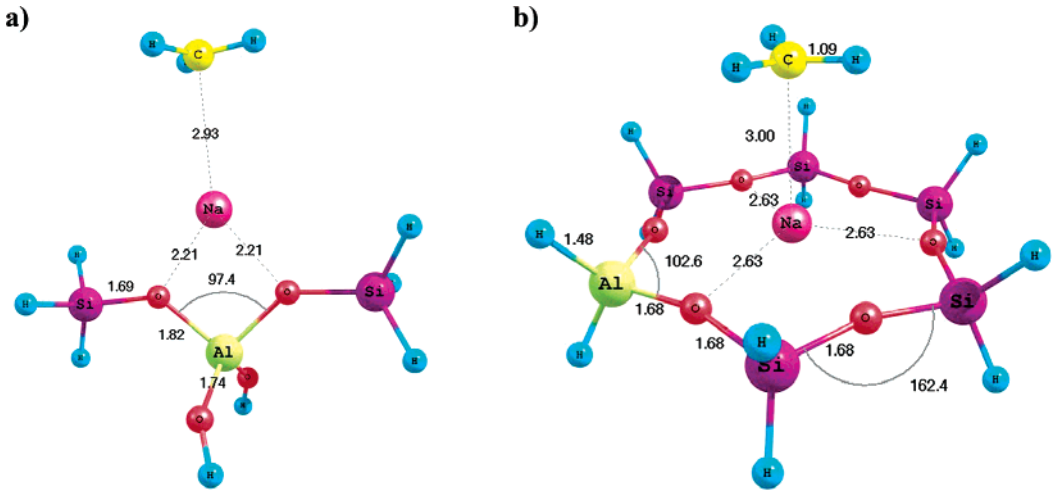

Figure 6. Two investigated theoretical models of the $^{\bullet}CH_3\cdots Na^+$ complex: (a) 3T cluster and b) six-membered (6T) ring with sodium cation and methyl radical. Geometries were optimized at the B3LYP/LANL2DZ theory level.

TABLE 1: Selected Structural Distance (Å) Parameters for the 3T Cluster and 6T Ring Models Obtained at the B3LYP/LANL2DZ Theory Level

distance	3T cluster	6T ring
Na−O	2.21	2.64
O−Si	1.69	1.68
O−Al	1.82	1.68
Na−C	2.93	3.0
C−H	1.09	1.09

TABLE 2: Calculated and Experimental H, Na, and ^{13}C Hyperfine Coupling Constants (all hfcc's in mT)

	3T cluster		6T ring		
	DGDZVP	DGA1	DGDZVP	DGA1	exptl
A(Na)	1.05	1.06	0.662	0.76	0.65
	EPR-III				
A(H)	2.05		2.1		2.29
A(^{13}C)	2.7		2.8		3.6

These results clearly show that EPR spectra obtained even in very similar zeolite/adsorbate systems strongly depend on the treatment method of zeolite and on the adsorption conditions.

Computational Results. Geometries of both optimized zeolite fragments—the 6T structure of one six-membered ring and the 3T cluster shown in Figure 6—are in pretty good agreement with previous literature data.[50−52] Table 1 summarizes the most important parameters, representative for the investigated model of zeolite-framework−$^{\bullet}CH_3\cdots Na^+$ interaction. All structural parameters of the $^{\bullet}CH_3\cdots Na^+$ complex are in good agreement with data obtained by Ghandi et al. for $^{\bullet}CH_3\cdots Na^+$ in NaY zeolite.[52] The 6T ring has been optimized with one of the Si atoms substituted by Al, since the presence of one or two Al atoms instead of Si in the six-membered ring could change the position of the sodium cation (Figure 6b). In this case the sodium cation remained in the center of the 6T ring, with the coordination number close to zero. The most recent crystallographic refinement of the LTA zeolite structure shows a possible Na^+ cation coordination with three oxygen atoms of the 6T ring, but despite this the sodium cation still occupies a nearly central position—shifted out of the center only by about 0.2 Å.[50,53] The van der Waals radius of the sodium cation is approximately the size of the 6T window, thus Na^+ can fit well inside, taking advantage of the stabilization in the center of the hexagonal window.

A comparison of the two applied models shows that the calculated distance between the methyl radical and the sodium cation in the 6T ring model is slightly longer than that in the 3T cluster. This seems to imply that the presence of the 6T ring does not affect the geometry of the methyl radical, which is known to be nearly planar. The angle between the plane perpendicular to the symmetry axis and the C−H bond of the methyl radical is less than 4°. Calculated hyperfine coupling constants for the optimized geometries are listed in Table 2. (Since the experimentally observed EPR spectra had an isotropic appearance we do not present anisotropic coupling constants obtained in the calculations.) The hyperfine coupling constants obtained for the Na and H atoms are in good agreement with those obtained experimentally. Especially, very good agreement has been obtained for *A*(Na) in the 6T ring model, which seems to more adequately mimic real experimental conditions than the 3T cluster.

The calculated ^{13}C hyperfine coupling constant (~2.7 mT) is much lower than the experimental value (3.85 mT), but, however, in good agreement with previous literature data.[54,55] Even at low temperatures methyl radicals can undergo significant vibrational motion. Chipman calculated that $A(^{13}C) \approx 2.7$ mT and $A(H) \approx 2.5$ mT for a $^{\bullet}CH_3$ radical, as compared to $A(^{13}C) = 3.8$ mT and $A(H) = 2.3$ mT, actually observed for the vibrating species.[56]

It is well-known that both *A*(H) and *A*(^{13}C) change gradually with increasing nonplanarity of the radical.[55,57] However, experimental and calculated hyperfine splitting constants strongly suggest that that both the free $^{\bullet}CH_3$ and $^{\bullet}CH_3$ interacting with a Na^+ cation have planar or nearly planar geometry.

The nearly planar structure predicted by the DFT calculations for the CH_3 unit makes it reasonable that the $^{\bullet}CH_3\cdots Na^+$ complexes trapped in α- and β-cages give similar ESR spectra. The H and ^{13}C hyperfine couplings should be nearly the same as for the "free" $^{\bullet}CH_3$ and similar between the complexes in α- and β-cages. Thus, except for the ^{23}Na hyperfine coupling the ESR parameters may not be strongly influenced by the surroundings in the present system.

Conclusions

The EPR results obtained for Na^+ and Li^+ exchanged zeolite clearly show that in γ-irradiated Na-A/CH_4 zeolites at least two types of methyl radicals are stabilized. At low temperatures (below 130 K) $^{\bullet}CH_3$ is placed close to Na^+ cations forming a $^{\bullet}CH_3\cdots Na^+$ complex. When Na-A zeolite is exposed to methane at room temperature those complexes are located only in α-cages and they are not stable above 130 K. On the contrary for zeolite

exposed to CH_4 at 413 K a portion of the $^{\bullet}CH_3\cdots Na^+$ complexes are stable at much higher temperatures. To explain this effect we postulate that at temperatures above 373 K methane molecules are able to penetrate through hexagonal windows to β-cages owing to the thermal motion of zeolite framework atoms.

The $^{\bullet}CH_3\cdots Na^+$ complexes located in α-cages decompose above 130 K and then the EPR spectrum of freely rotating $^{\bullet}CH_3$ radicals is recorded. In zeolites exposed at room temperature to 0.4 kPa of CH_4 methyl radicals are effectively isolated by cavity walls from other molecules and remain stable until 280 K. When CH_4 adsorption is carried out above 373 K free $^{\bullet}CH_3$ radicals in α-cages coexist in the temperature range 130−280 K with $^{\bullet}CH_3\cdots Na^+$ complexes trapped inside β-cages. This agrees with earlier reports on similar systems and clearly indicates that the treatment of zeolite before exposure to adsorbate molecules plays a crucial role for the location of the $^{\bullet}CH_3$ radicals and their interaction with zeolite atoms.

References and Notes

(1) Iu, K. K.; Liu, X.; Thomas, J. K. *J. Phys. Chem.* **1993**, *97*, 8165.
(2) Michalik, J.; Zamadics, M.; Sadlo, J.; Kevan, L. *J. Phys. Chem.* **1993**, *97*, 10440.
(3) Chemerisov, S. D.; Werst, D. W.; Trifunac, A. D. *Chem. Phys. Lett.* **1998**, *291*, 262.
(4) Liu, X.; Dilger, H.; Eichel, R. A.; Kunstmann, J.; Roduner, E. *J. Phys. Chem. B* **2006**, *110*, 2013.
(5) Marti, F.; Fernandez, L.; Fornes, V.; Garcia, H.; Roth, H. D. *J. Chem. Soc., Perkin Trans. 2* **1999**, *2*, 145.
(6) Qin, X. Z.; Trifunac, A. D. *J. Phys. Chem.* **1990**, *94*, 4751.
(7) Yamazaki, T.; Watanuki, I.; Ozawa, S.; Ogino, Y. *Langmuir* **1988**, *4*, 433.
(8) Yamazaki, T.; Hasegawa, K.; Honma, K.; Ozawa, S. *Phys. Chem. Chem. Phys.* **2001**, *2*, 2686.
(9) Figueroa, O. L.; Lee, C.; Akbar, S. A.; Szabo, N. F.; Trimboli, J. A.; Dutta, P. K.; Sawaki, N.; Soliman, A. A.; Verweij, H. *Sens. Actuators, B* **2005**, *107*, 839.
(10) Corma, A. *Catal. Lett.* **1993**, *22*, 33.
(11) Kasai, P. H.; McLeod, D. *J. Am. Chem. Soc.* **1972**, *94*, 7975.
(12) Lee, H.; Kevan, L. *J. Phys. Chem.* **1986**, *90*, 5781.
(13) Shiga, T.; Lund, A. *J. Phys. Chem.* **1973**, *77*, 453.
(14) Joppien, G. R.; Willard, J. E. *J. Phys. Chem.* **1972**, *78*, 3158.
(15) Katsu, T.; Yanagita, M.; Fujita, Y. *J. Phys. Chem.* **1971**, *75*, 4064.
(16) Fujimoto, M.; Gesser, H. D.; Garbutt, B.; Cohen, A. *Science* **1966**, *154*, 381.
(17) Shiga, T.; Yamada, H.; Lund, A. *Z. Naturforsch.* **1974**, *29a*, 653.
(18) Fessenden, R. W.; Schuler, R. H. *J. Chem. Phys.* **1963**, *39*, 2147.
(19) Garbutt, B.; Gesser, H. D. *Can. J. Chem.* **1970**, *48*, 2685.
(20) Kubota, S.; Iwaizumi, M.; Isobe, T. *Bull. Chem. Soc. Jpn.* **1971**, *44*, 2684.
(21) Yamada, T.; Komaguchi, K.; Shiotani, M.; Benetis, N. P.; Sornes, A. R. *J. Phys. Chem.* **1999**, *103*, 4823.
(22) Noble, G. A.; Serway, R. A.; O'Donell, A.; Freeman, E. S. *J. Phys. Chem.* **1967**, *71*, 4326.
(23) Shiotani, M.; Yuasa, F.; Sohma, J. *J. Phys. Chem.* **1975**, *79*, 2669.
(24) Stevens, G. C.; Clarke, R. M.; Hart, E. J. *J. Phys. Chem.* **1972**, *76*, 3863.
(25) Blaszkowski S. R.; Jansen, A. P. J.; Nascimento, M. A. C.; van Santen, R. A. *J. Phys. Chem.* **1994**, *98*, 12938.
(26) Hunger, M.; Horvath, T. *J. Am. Chem. Soc.* **1996**, *118*, 12302.
(27) Truong, T. N. *J. Phys. Chem. B* **1997**, *101*, 2750.
(28) Vollmer, J. M.; Truong, T. N. *J. Phys. Chem. B* **2000**, *104*, 6308.
(29) Danilczuk, M.; Pogocki, D.; Lund, A.; Michalik, J. *Phys. Chem. Chem. Phys.* **2004**, *6*, 1165.
(30) Corma, A.; Sastre, G.; Viruela, P. M. *J. Mol. Catal. A: Chem.* **1995**, *100*, 75.
(31) Okulik, N. B.; Diez, R. P.; Jubert, A. H. *Comput. Mater. Sci.* **2000**, *17*, 88.
(32) Pietrzyk, P.; Sojka, Z. *J. Phys. Chem. A* **2005**, *109*, 10571.
(33) Plant, D. F.; Simperler, A.; Bell, R. G. *J. Phys. Chem. B* **2006**, *110*, 6170.
(34) O'Malley, P. J.; Collins, S. J. *Chem. Phys. Lett.* **1996**, *259*, 296.
(35) O'Malley, P. J. *J. Phys. Chem. A* **1997**, *101*, 6334.
(36) O'Malley, P. J. *J. Phys. Chem. A* **1997**, *101*, 9813.
(37) O'Malley, P. J. *J. Phys. Chem. A* **1998**, *102*, 248.
(38) O'Malley, P. J.; Farnworth, K. J. *J. Phys. Chem. B* **1998**, *102*, 4507.
(39) O'Malley, P. J. *Chem. Phys. Lett.* **2000**, *325*, 69.
(40) Barone, V. In *Recent Advances in Density Functional Methods*, Part I, D. P. Chong, D. P., Ed.; World Scientific Publ. Co., Singapore, 1996.
(41) Becke, A. D. *J. Chem. Phys.* **1993**, *98*, 5648.
(42) Dunning, T. H.; Hay, P. J. *Modern Theoretical Chemistry*; Schaefer, H. F., III, Ed.; Plenum: New York, 1976; pp 1−28.
(43) Hay, P. J.; Wadt, W. R. *J. Chem. Phys.* **1985**, *82*, 284.
(44) Hay, P. J.; Wadt, W. R. *J. Chem. Phys.* **1985**, *82*, 299.
(45) Frisch, M. J.; et al. *Gaussian 98*, Rev. A.7; Gaussian Inc.: Pittsburgh, PA, 1998.
(46) Baerlocher, Ch.; Meier, W. M.; Olson, D. H. *Atlas of Zeolite Framework Types*, 5th revised ed.; Elsevier: Amsterdam, The Netherlands, 2001.
(47) Stamires, D. N.; Turkevich, J. *J. Am. Chem. Soc.* **1964**, *86*, 749.
(48) Lim, W. T.; Park, M.; Heo, N. H. *Bull. Korean Chem. Soc.* **2000**, *21*, 75.
(49) Heo, N. H.; Lim, W. T.; Kim, B. J.; Lee, S. Y.; Kim, M. C.; Seff, K. *J. Phys. Chem. B* **1999**, *103*, 1881.
(50) Pluth, J. J.; Smith, J. V. *J. Am. Chem. Soc.* **1980**, *102*, 4704.
(51) Yanagida, R. Y.; Amaro, A. A.; Seff, K. *J. Phys. Chem.* **1973**, *77*, 805.
(52) Ghandi, K.; Zahariev, F. E.; Wang, Y. A. *J. Phys. Chem. A* **2005**, *109*, 7242.
(53) Liu, Y.-J.; Lund, A.; Persson, P.; Lunell, S. *J. Phys. Chem. B* **2005**, *109*, 7948.
(54) Eriksson, L. A.; Malkina, O. L.; Malkin, V. G.; Salahub, D. R. *J. Chem. Phys.* **1994**, *100*, 5066.
(55) Tachikawa, H.; Igarashi, M.; Ishibashi, T. *Chem. Phys. Lett.* **2002**, *352*, 113.
(56) Chipman, D. M. *J. Chem. Phys.* **1983**, *78*, 3112.
(57) Dolbier, W. R., Jr. *Chem. Rev.* **1996**, *96*, 1557.